International Journal of Mass Spectrometry 309 (2012) 133–140

Contents lists available at SciVerse ScienceDirect

International Journal of Mass Spectrometry

journal homepage: www.elsevier.com/locate/ijms

Fragmentation study of five trichothecenes using electrospray hybrid ion trap/time-of-flight mass spectrometry with accurate mass measurements

Zhao-Ying Liu[a], Chun-Hong Yu[a], Leren Wan[b], Zhi-Liang Sun[a,*]

[a] Biological Veterinary Drugs Branch, National Research Center of Engineering & Technology for Utilization of Botanical Functional Ingredients, College of Veterinary Medicine, Hunan Agricultural University, Changsha, Hunan, 410128 China
[b] Shimadzu International Trading (Shanghai) Co., Limited, Shanghai 200052, China

ARTICLE INFO

Article history:
Received 11 August 2011
Received in revised form
14 September 2011
Accepted 14 September 2011
Available online 21 September 2011

Keywords:
Trichothecenes
Ion trap/time-of-flight mass spectrometry
Accurate mass
Fragmentation

ABSTRACT

Five trichothecenes, T-2 toxin, HT-2 toxin, deoxynivalenol (DON), 3-acetyl-DON (3-AcDON) and nivalenol (NIV), major class of mycotoxins produced by *Fusarium*, were investigated by electrospray hybrid ion trap/time-of-flight mass spectrometry (IT–TOF-MS). Fragmentation mechanisms are proposed based on the MS^2 and MS^3 experiments and accurate mass measurements. The sodium adduct ions $[M+Na]^+$ of type-A trichothecenes, such as T-2 toxin and HT-2 toxin, were observed in the MS spectra. However, the $[M-H]^-$ ions of type-B trichothecenes, such as NIV, and 3-AcDON, were observed in the MS spectra. Eliminations of isovaleryloxy group and acetic acid were the common fragmentation pathways of T-2 toxin and HT-2 toxin. However, the cleavage of epoxy was the common fragmentation pathways of DON, 3-AcDON and NIV. The other fragmentation pathways were found to be dependent on the substitutent group. The data reported here may help to identify analogues of the trichothecenes that are commonly co-produced by *Fusarium* in cultures or naturally contaminated samples.

1. Introduction

The trichothecene mycotoxins are secondary metabolites of some species in the fungal genera *Fusarium*, *Myrothecium*, *Trichothecium* and *Cephalosporium*. A large number of different trichothecene analogues have been isolated and characterized from various fungi [1]. The trichothecenes as a group are based on the same basic chemical structure, a 12, 13-epoxytrichothec-9-ene ring system. The group is subdivided four types (A–D) according to structural similarities. However, the type-A and -B trichothecenes are common in grain as a result of infection with *Fusarium*, and are therefore often contaminants of food and feed. Type-A trichothecenes have an ester bond at C-8, while the type-B trichothecenes possess a ketone group at C-8.

In cereal grains, T-2 toxin and HT-2 toxin are regarded as the most important type-A trichothecenes, while deoxynivalenol (DON), and its 3-acetyl-derivative (3AcDON) as well as nivalenol (NIV) are regarded as the most important type-B trichothecenes (Fig. 1). These trichothecenes possess a potent cytotoxicity to eukaryotic cells, and this biological activity is closely related to their lethal toxicity, dermal toxicity, cellular damage to actively dividing cells, impairment of immunoresponses, and inhibition of macromolecule syntheses [2]. Thus, when the potential food safety problem and their various toxic effects are grasped, the accurate and convenient determination of the foods contaminated with these toxins is important for the supply of safe foods.

Many methodologies for the routine analysis of the most common trichothecenes based on gas chromatography/mass spectrometry (GC/MS) have been published [3,4]. These consist in general of four steps: extraction, clean up, derivatization and instrumental analysis. There are also a few reports on the electron ionization (EI) mass spectrometric analysis of the fragmentation of the trichothecenes [5,6]. However, these trichothecenes are nowadays often analyzed using liquid chromatography/mass spectrometry (LC/MS) [7,8]. In addition to being well suited for the quantification of fungal metabolites in most matrices, LC/MS can give structural information and thus help to identify known compounds without derivatization. However, there is a lack of detailed studies on the fragmentation behaviour of these trichothecenes in the electrospray ionization.

As one of the latest LC/MS instrumentation designs, hybrid ion trap/time-of-flight mass spectrometry (IT–TOF/MS) is effective for the structural analysis of organic compounds. This hybrid instrument has the ability to provide multistage tandem spectra (MS^{1-10}) with accurate masses (error <5 mDa) in both MS and MS^n modes. With this technique, we can acquire much reliable structural information about the product ions, based on the exact masses and the multistage tandem mass spectrometric analyses [9,10].

* Corresponding author at: College of Veterinary Medicine, Hunan Agricultural University, Furong District, Changsha 410128, Hunan, China.
Tel.: +86 731 84635229; fax: +86 731 84673618.
E-mail address: sunzhiliang1965@yahoo.com.cn (Z.-L. Sun).

1387-3806/$ – see front matter © 2011 Elsevier B.V. All rights reserved.
doi:10.1016/j.ijms.2011.09.007

Table 1
The elemental composition, accurately measured mass/charge ratio and theoretical mass/charge ratio, double bond equivalents (DBE), the mass errors expressed in milli-Daltons and parts-per-million of the trichothecenes.

Compound	Mode	Elemental composition	Accurately measured mass/charge ratio (Th)	DBE	Theoretical mass/charge ratio (Th)	Error (mDa)	Error (ppm)
T-2 toxin	$[M+Na]^+$	$C_{24}H_{34}O_9Na^+$	489.2108	8	489.2095	1.3	2.66
HT-2 toxin	$[M+Na]^+$	$C_{22}H_{32}O_8Na^+$	447.1995	8	447.1989	0.6	1.34
DON	$[M-H]^-$	$C_{15}H_{19}O_6^-$	295.1191	6	295.1187	0.4	1.36
3-AcDON	$[M-H]^-$	$C_{17}H_{21}O_7^-$	337.1283	7	337.1293	−1.0	−2.97
NIV	$[M-H]^-$	$C_{15}H_{19}O_7^-$	311.1121	6	311.1136	−1.5	−4.82

Table 2
The elemental composition, accurately measured mass/charge ratio and theoretical mass/charge ratio, double bond equivalents (DBE), the mass errors expressed in milli-Daltons and parts-per-million of product ions observed in the MS^2 and MS^3 spectra for $[M+Na]^+$ of T-2 toxin.

Elemental composition	Measured mass/charge ratio (Th)	Theoretical mass/charge ratio (Th)	DBE	Error (mDa)	Error (ppm)
$C_{22}H_{30}O_7Na^+$	429.1882	429.1884	8.0	−0.2	−0.47
$C_{19}H_{24}O_7Na^+$	387.1421	387.1414	8.0	0.7	1.81
$C_{17}H_{22}O_6Na^+$	345.1345	345.1309	7.0	3.6	10.43
$C_{17}H_{20}O_5Na^+$	327.1208	327.1203	8.0	0.5	1.53
$C_{15}H_{17}O_3Na^+$	268.1059	268.1070	7.5	−1.1	−4.10
$C_{15}H_{16}O_3Na^+$	267.0980	267.0992	8.0	−1.2	−4.49
$C_{13}H_{18}O_3Na^+$	245.1168	245.1128	5.0	2.0	8.16
$C_{11}H_{16}Na^+$	171.1155	171.1144	4.0	1.1	6.43
$C_{11}H_{14}ONa^+$	185.0943	185.0937	5.0	0.6	3.24

Table 3
The elemental composition, accurately measured mass/charge ratio and theoretical mass/charge ratio, double bond equivalents (DBE), the mass errors expressed in milli-Daltons and parts-per-million of product ions observed in the MS^2 and MS^3 spectra for $[M+Na]^+$ of HT-2 toxin.

Elemental composition	Measured mass/charge ratio (Th)	Theoretical mass/charge ratio (Th)	DBE	Error (mDa)	Error (ppm)
$C_{20}H_{28}O_6Na^+$	387.1816	387.1778	7.0	3.8	9.81
$C_{17}H_{22}O_6Na^+$	345.1314	345.1309	7.0	0.4	1.16
$C_{17}H_{20}O_5Na^+$	327.1200	345.1203	7.0	−0.3	−0.92
$C_{16}H_{20}O_5Na^+$	315.1212	315.1203	7.0	0.9	2.86
$C_{15}H_{20}O_4Na^+$	287.1261	287.1254	6.0	0.7	2.44
$C_{15}H_{18}O_4Na^+$	285.1108	285.1097	7.0	1.1	3.86
$C_{14}H_{16}O_3Na^+$	255.0988	255.0992	7.0	−0.4	−1.57
$C_{13}H_{16}O_2Na^+$	227.1047	227.1067	6.0	0.4	1.76
$C_{12}H_{14}O_2Na^+$	213.0866	213.0886	6.0	−2.0	−9.39
$C_{11}H_{11}Na^+$	166.0771	166.0753	6.5	1.8	10.84

Therefore, the aim of the present work described in this paper was to use IT–TOF/MS to study the fragmentation behaviour of five trichothecenes, T-2 toxin, HT-2 toxin, DON, NIV and 3-AcDON. The elucidation of fragmentation pathways of these trichothecenes was based on their multistage tandem mass spectrometry and accurate mass measurements. To our knowledge, this is the first report of the complete characterization of the fragmentation of these trichothecenes using IT–TOF/MS with accurate mass measurements.

2. Experimental

2.1. Materials

T-2 toxin, HT-2 toxin, DON, NIV and 3-AcDON were obtained from Sigma (St. Louis, USA). HPLC-grade acetonitrile was purchased from Fisher Chemicals Co. (NJ, USA). Water was freshly prepared with the Millipore water purification system (MA, USA). Sample solutions were prepared by dissolving in acetonitrile and then further diluted to a final the concentration of 100 mg L^{-1} or less with 50/50 acetonitrile/water prior to mass spectrometric analysis.

2.2. Mass spectrometry

All mass spectra were acquired on a hybrid ion trap/time-of-flight mass spectrometer (Shimadzu Corp., Kyoto, Japan) equipped with an electrospray ionization source (ESI-IT–TOF/MS). The samples were introduced into the source via a syringe pump at a flow rate of 5 μL min^{-1}. In order to get the abundant signal for the product ion scan, the full scan MS of the trichothecenes were acquired in the both positive ion mode and negative ion mode. Mass spectrometric analysis was carried out on full-scan MS with a mass range of 100–500 Th. The relevant precursor ions were selected for collision-induced dissociation (CID) tandem mass spectrometric analysis. For the MS^3 product ion scan analysis with multiple peaks, two second-generation product ions were usually selected as precursor ions. The first one is the product ion with the higher mass (excluding the peaks with relative intensities below 5%); the second is the product ion with the greatest signal intensity (base peak).

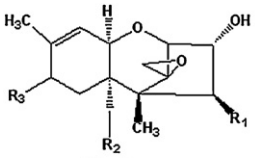

Type-A trichothecenes

	R_1	R_2	R_3
T-2 toxin	OAc	OAc	$OCOCH_2CH(CH_3)_2$
HT-2 toxin	OH	OAc	$OCOCH_2CH(CH_3)_2$

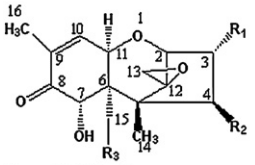

Type-B trichothecenes

	R_1	R_2	R_3
Deoxynivalenol(DON)	OH	H	OH
Nivalenol	OH	OH	OH
3-acetyl-DON	OAc	H	OH

Fig. 1. The structures for the trichothecenes studied.

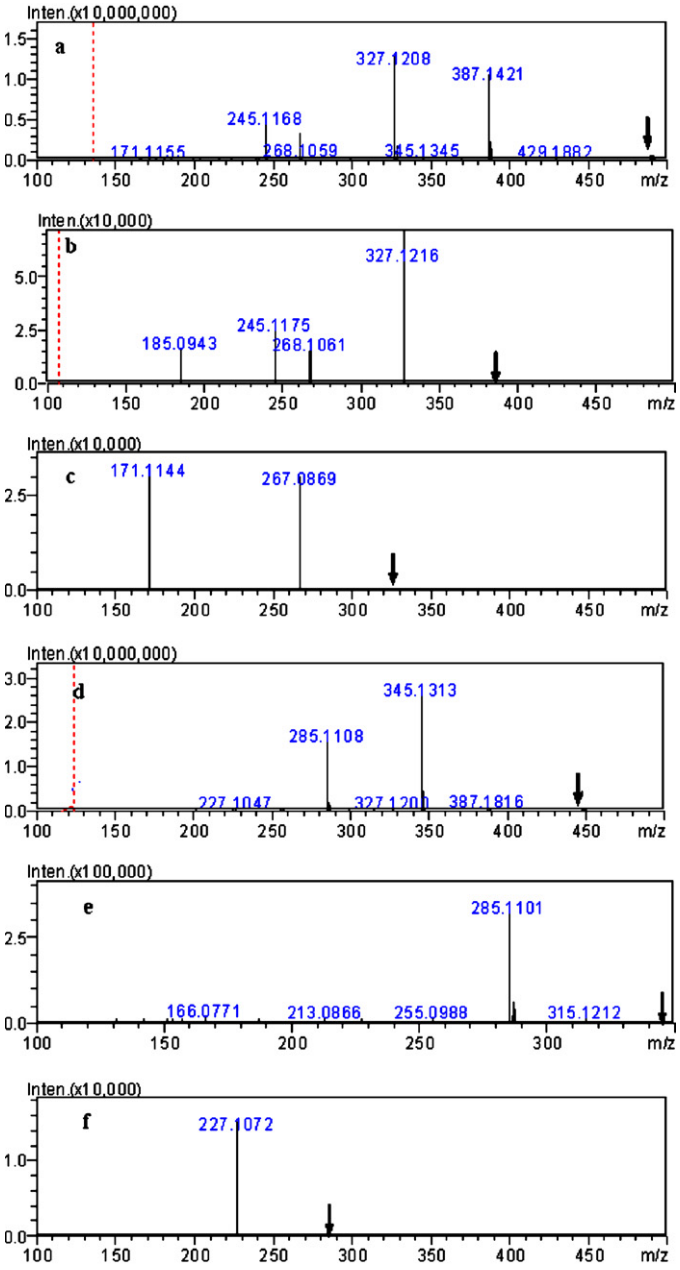

Fig. 2. The accurate MS^{2-3} spectra of sodium adduct ion $[M+Na]^+$ of T-2 toxin (a, MS^2 of m/z 489; b, MS^3 of m/z 489 → 387; c, MS^3 of m/z 489 → 327), and HT-2 toxin (d, MS^2 of m/z 447; e, MS^3 of m/z 447 → 345; f, MS^3 of m/z 447 → 285). The vertical arrow in each panel indicates the precursor ion mass/charge ratio.

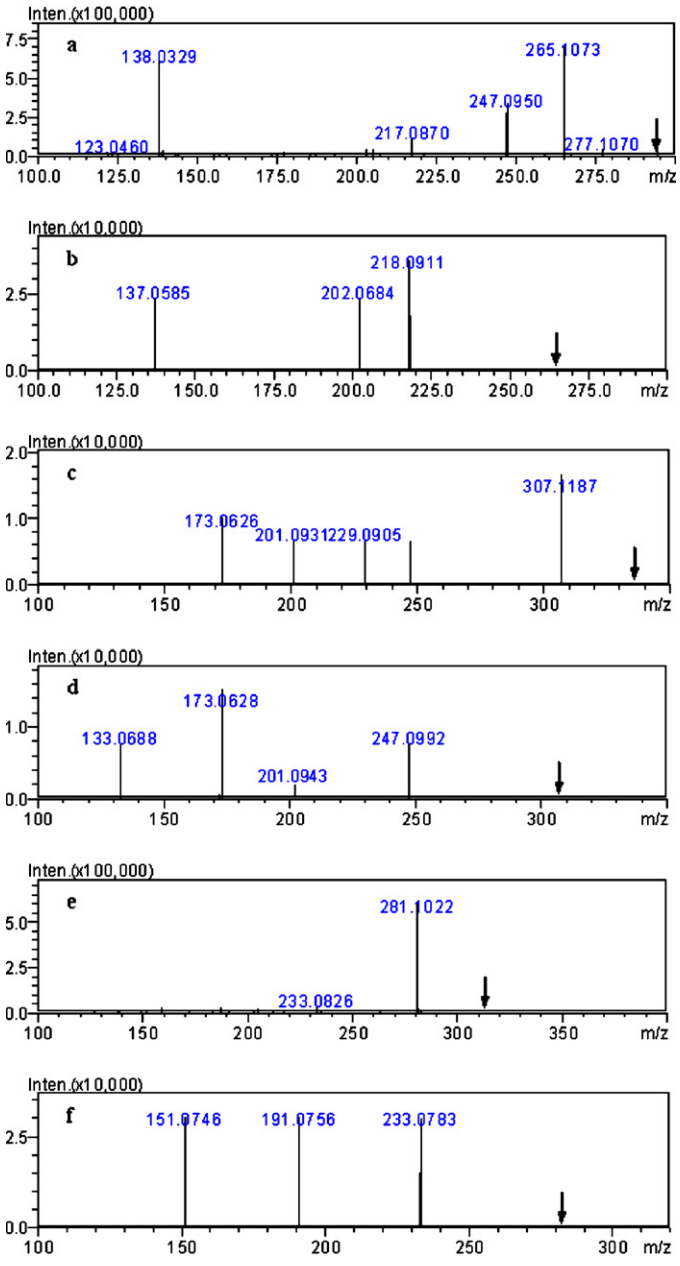

Fig. 3. The accurate MS^{2-3} spectra of $[M-H]^-$ ion of DON (a, MS^2 of m/z 295; b, MS^3 of m/z 295 → 265), 3-AcDON (c, MS^2 of m/z 337; d, MS^3 of m/z 337 → 307), and NIV (e, MS^2 of m/z 311; f, MS^3 of m/z 311 → 281). The vertical arrow in each panel indicates the precursor ion mass/charge ratio.

For positive ion mode, the spray and detector voltages were set at 4.5 kV and 1.7 kV, respectively. However, the spray and detector voltages were set at −3.5 kV and 1.65 kV for the negative ion, respectively. Nitrogen was used as the nebulizing gas at a flow rate of 1.5 L min^{-1}. The curved desolvation line (CDL) and heat block temperatures were both maintained at 200 °C. The MS^2 and MS^3 spectra were produced using CID of the selected precursor ions using argon as collision gas with relative energy of 25% and 50%, respectively. The ion accumulation time was set at 50 ms, the precursor ion isolation width at 1 Th (positive ion mode) or 3 Th (negative ion mode). External mass calibration was carried out prior to data acquisition using direct infusion of a reference standard from 50 to 1000 Th. The reference standard consisted of 0.25 mL L^{-1} trifluoroacetic acid and 0.1 g L^{-1} sodium hydrate.

2.3. Formula assignments

Accurate masses of all fragment ions were processed using the LC/MS solution version 3.41 software supplied with the instrument. Any mass numbers corresponding to particular elemental compositions were also calculated by the formula predictor, and would generate more than one formula proposed by the software. To assign the elemental composition of fragment ions, the error ranges were set less than 5 mDa as a limit to the calculation of possible elemental compositions using the formula predictor. The other following conditions for calculating elemental compositions were taken into consideration: the upper limits on the number of C, H, O atoms, C/H ratios and range of double-bond-equivalent (DBE).

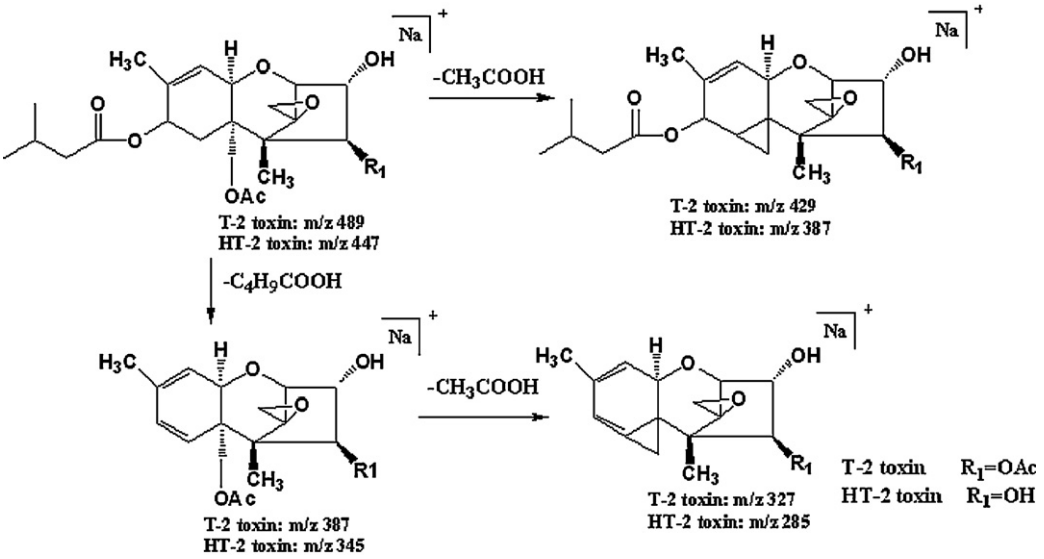

Scheme 1. The similar fragmentation mechanism proposed for the sodium adduct ion $[M+Na]^+$ of T-2 toxin and HT-2 toxin.

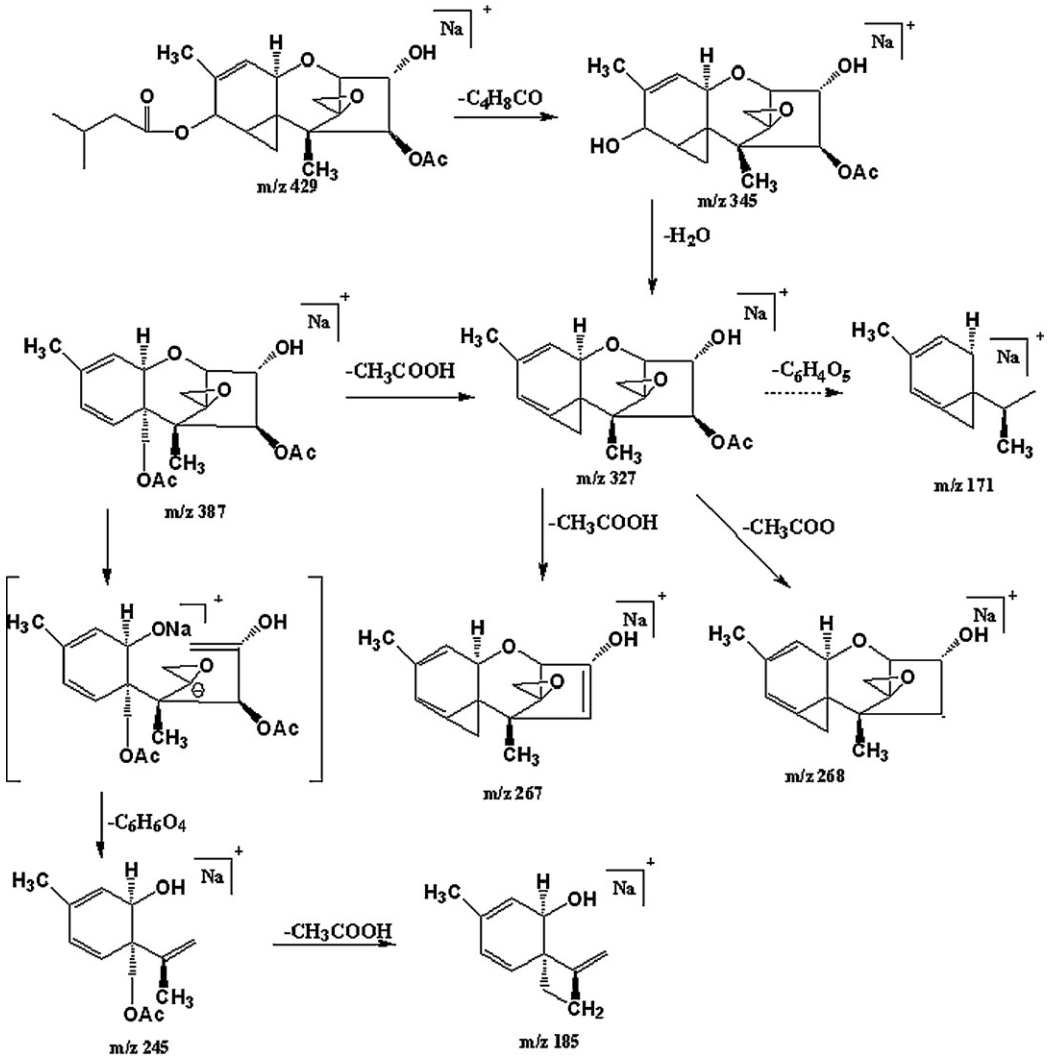

Scheme 2. The additional fragmentation mechanism proposed for the sodium adduct ion $[M+Na]^+$ of T-2 toxin.

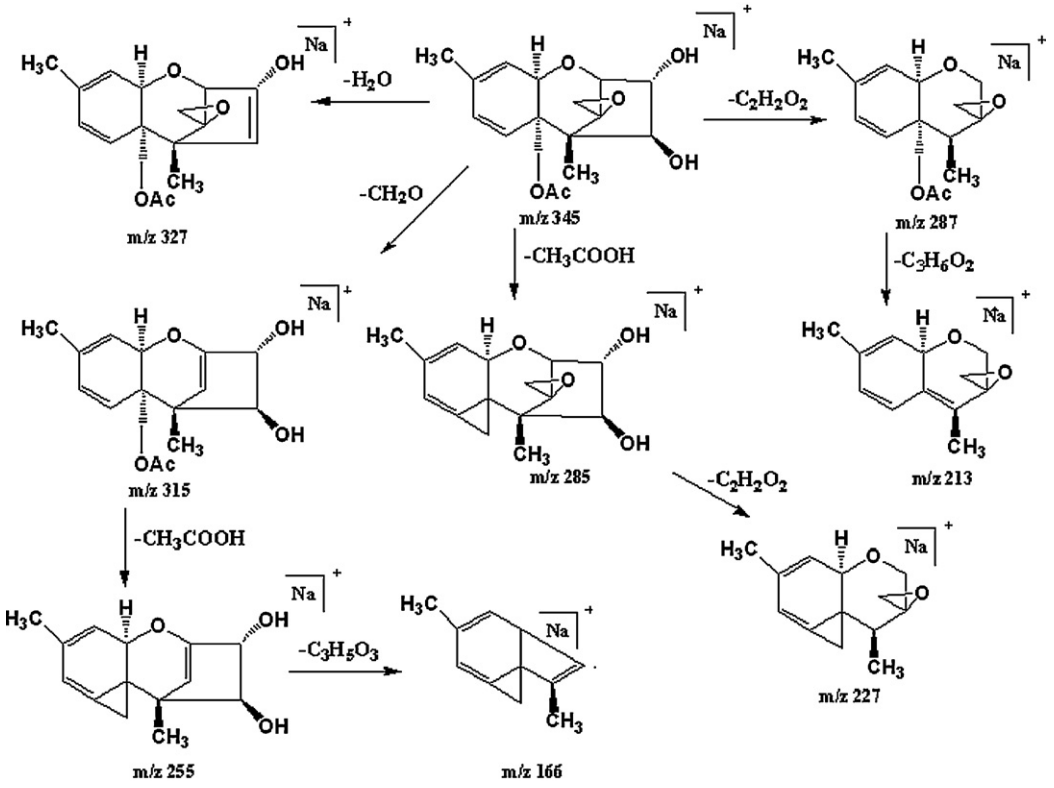

Scheme 3. The additional fragmentation mechanism proposed for the sodium adduct ion $[M+Na]^+$ of HT-2 toxin.

3. Results and discussion

The mass spectra[2–3] of the type-A trichothecenes were obtained only in positive ion mode because the ion signal intensities in negative ion mode were so low (data not shown). The sodium adduct ion $[M+Na]^+$ of T-2 toxin and HT-2 toxin were observed in the mass spectra obtained with the ESI-IT–TOF. On the other hand, the type-B trichothecenes showed the low ion signal intensities for positive ions, such that for these compounds, mass spectral data were obtained only in the negative ion mode. The $[M-H]^-$ ions of DON, NIV, and 3-AcDON were observed in the mass spectra obtained with the ESI-IT–TOF. The elemental composition, accurately measured mass/charge ratio and theoretical mass/charge ratio, the mass errors expressed in milli-Daltons (mDa) and parts-per-million (ppm) of the trichothecenes are indicated in Table 1. The exact and measured mass/charge ratios agree to within ±2 mDa or 5 ppm for trichothecenes, providing support for the proposed elemental compositions of these compounds.

3.1. Fragmentations of type-A trichothecenes

The accurate MS^2 and MS^3 spectra of T-2 toxin and HT-2 toxin are shown in Fig. 2. Accurately measured mass/charge ratio and corresponding assigned elemental composition of product ions from the MS^2 and MS^3 spectra of T-2 toxin and HT-2 toxin are summarized in Tables 2 and 3, respectively. The errors between measured and predicted values of the product ions of T-2 toxin and HT-2 toxin ranged from −2.0 to 3.6 mDa (−9.39 to 10.84 ppm), indicated relatively good accuracy. It should be noted that a mass accuracy with ±5 mDa for an ion of *m*/*z* 500, there are few different elemental composition that satisfy the requirements of the elemental composition of the known parent ion.

Based on the predicated elemental compositions and the structure of parent drug, the structures of product ions can be obtained with a high degree of confidence. According the ESI-MS^2 results of *m*/*z* 489 and 447, the two compounds had similar fragmentation behaviour (Scheme 1). Both compounds can lose easily isovaleryloxy group as acid (C_4H_9COOH, −102 Da) yielding the abundant ions at *m*/*z* 387 and 345 for T-2 toxin and HT-2 toxin, respectively. However, the sodium adduct ion $[M+Na]^+$ of T-2 toxin and HT-2 toxin can also lose the acetic acid (CH_3COOH, −60 Da) yielding very low abundant ions at *m*/*z* 429 and 387, respectively. This suggested that the elimination of the longer acyl chains of type-A trichothecenes is preferred over cleavage of the acetyl. These ions, *m*/*z* 387 for T-2 toxin and *m*/*z* 345 for HT-2 toxin, can lose another acetic acid (CH_3COOH, −60 Da) to generate the ions at *m*/*z* 327 (T-2 toxin) and *m*/*z* 285 (HT-2 toxin). Taking into account the structures of the both compounds, for T-2 toxin the loss of acetic acid can occur at C15 or C4, whereas for HT-2 toxin this loss can only occur at C15. Therefore, the loss of acetic acid of type-A trichothecenes can occur easily at position C-15. These fragmentations were confirmed by their MS^3 spectra.

As for the T-2 toxin, the loss of C_4H_8CO (−84 Da) from the ion *m*/*z* 429 lead to a low abundant product ion at *m*/*z* 345, which indicates the elimination of the isovaleryloxy group at C-8 as ketene. The ion at *m*/*z* 345 can further lose H_2O to afford the ion at *m*/*z* 327. In the MS^3 spectrum of precursor ion at *m*/*z* 387 (see Fig. 2(b)), the product ions at *m*/*z* 268 and 267 were formed by the elimination of $CH_3COO\cdot$ radical and CH_3COOH from *m*/*z* 327, respectively. The fragment pattern was confirmed by the MS^3 spectrum of precursor ion at *m*/*z* 327(see Fig. 2(c)). The elemental composition of the product ion at *m*/*z* 245.1168 was $C_{13}H_{18}O_3Na$ (predicted 245.1148 Da), according to the formula predictor software, indicating that $C_6H_6O_4$ was lost from *m*/*z* 387 to form *m*/*z* 245. The ion at *m*/*z* 387 would form the intermediate which initially would undergo scission of the pyran rings at the bond C2–O. The structure of ion at *m*/*z* 245 might derive from the cleavage of intermediate at the bond C4–C5 and the epoxy. The ion at *m*/*z* 185 was formed by the loss of acetic

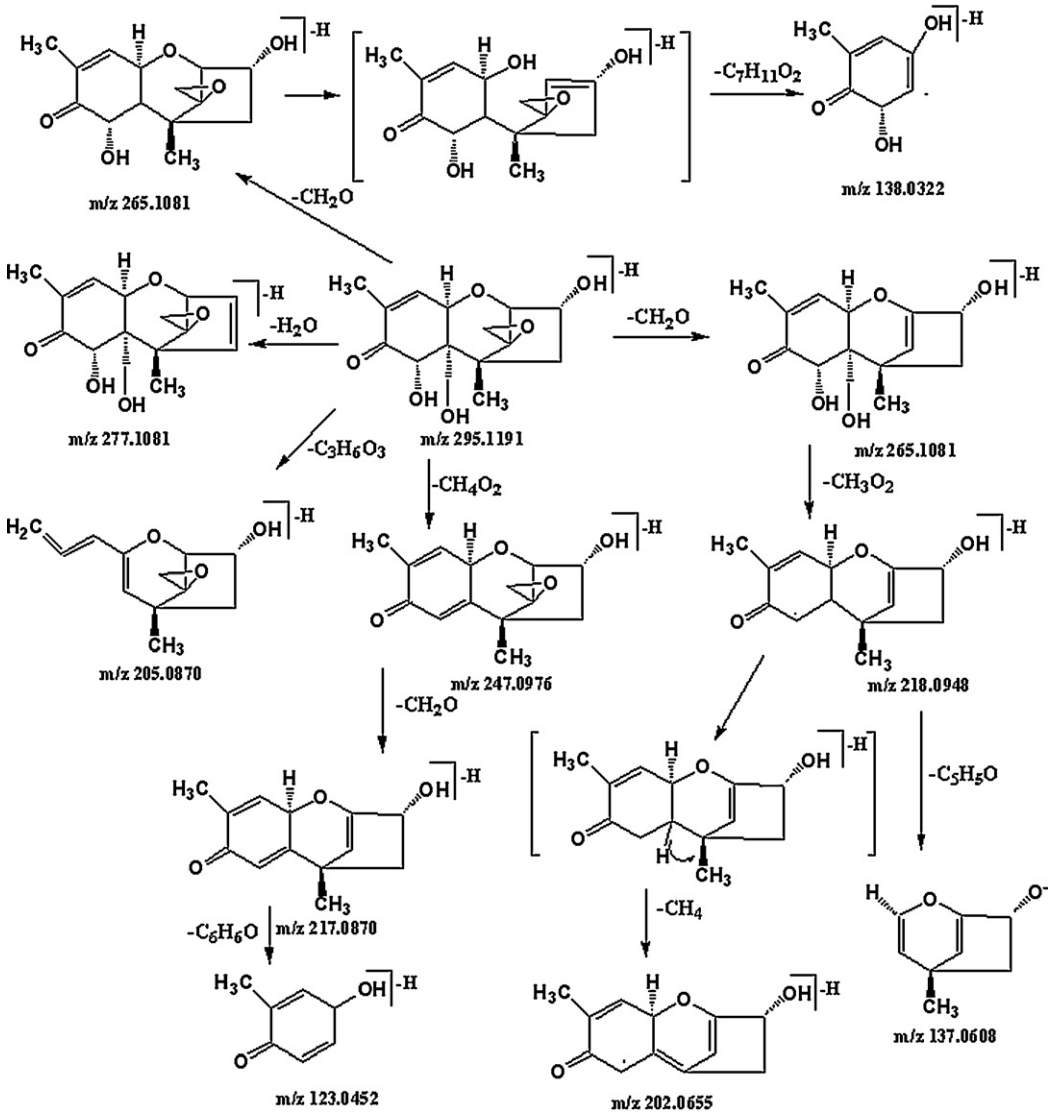

Scheme 4. The proposed fragmentation pathways for deprotonated ion $[M-H]^-$ of DON.

acid (CH_3COOH, −60 Da) from *m*/*z* 245. A low intensity product ion at *m*/*z* 171.1144 derived an empirical formula of $C_{11}H_{16}Na$, according to the formula predictor software, and this ion was thought to arise from the *m*/*z* 327 via severe cleavages and rearrangements of epoxy and cycloalkane ring.

As for the HT-2 toxin, in addition to the product ions at *m*/*z* 345 and 285, there are other low intensity production ions in Fig. 2(d). The low relative abundances of these ions indicate that their formations are minor fragmentation pathways for the HT-2 toxin. A low abundant product ion at *m*/*z* 327 was formed by the loss of H_2O at cycloalkane ring from the ion at *m*/*z* 345. The product ion at *m*/*z* 315 existed in the MS^3 spectrum of *m*/*z* 345 (see Fig. 2(e)), which suggests the elimination of epoxy at the position C-12. The ion could lose another acetic acid molecule (CH_3COOH, −60 Da) to generate the ion at *m*/*z* 255. In the MS^3 spectrum of precursor ion at *m*/*z* 345, the low abundant product ion at *m*/*z* 227 was formed by the cleavage of the cycloalkane ring at positions C2-3 and C4-5 from *m*/*z* 285. The fragment pattern was also confirmed by the MS^3 spectrum of precursor ion at *m*/*z* 285(see Fig. 2(f)). The cleavage of the cycloalkane ring at positions C2-3 and C4-5 of the ion at *m*/*z* 345 generated the product ion at *m*/*z* 287. On the basis of accurate mass measurement, the elemental composition of the low intensity product ion at *m*/*z* 213.0866 was $C_{12}H_{14}O_2Na$ (predicted 213.0886 Da). The ion was believed to arise from *m*/*z* 287 via the cleavage of the methyl acetate at the position C-6. A low intensity product ion at *m*/*z* 166.0771 derived an empirical formula of $C_{11}H_{11}Na$, according to the formula predictor software, and this ion was thought to arise from the *m*/*z* 255 via severe cleavages and rearrangements of cycloalkane ring.

The observations described are summarized in Schemes 2 and 3 which depicts the additional fragmentation mechanism proposed for the sodium adduct ion $[M+Na]^+$ of T-2 toxin and HT-2 toxin, respectively.

3.2. Fragmentations of type-B trichothecenes

The ESI-MS^{2-3} spectra of deprotonated molecule of DON, 3-AcDON and NIV are presented in Fig. 3(a)–(f). Accurately measured mass/charge ratio and corresponding assigned elemental composition of product ions from the MS^2 and MS^3 spectra of deprotonated molecule of DON, 3-AcDON and NIV are summarized in Tables 4–6, respectively. The three deprotonated compounds can lose easily CH_2O (−30 Da) affording the most abundant ions at *m*/*z* 265, 307 and 281 for DON, 3-AcDON and NIV, respectively. Taking into account the structures of these compounds, the loss of CH_2O is the cleavage of epoxy at the position C-12.

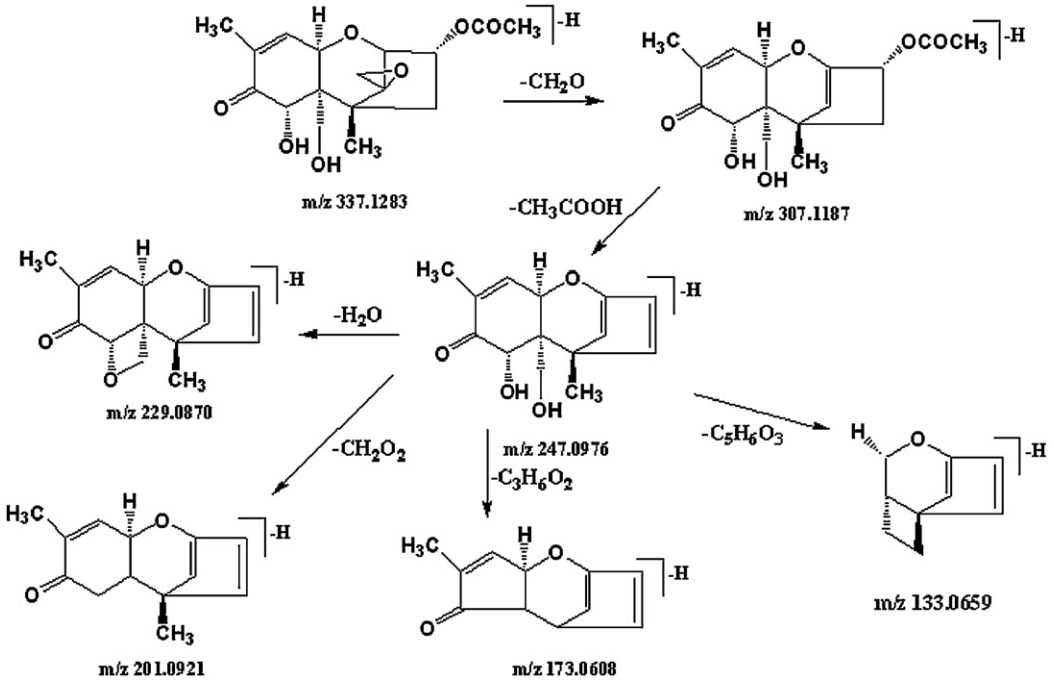

Scheme 5. The proposed fragmentation pathways for deprotonated ion $[M-H]^-$ of 3-AcDON.

For DON the loss of H_2O from the deprotonated molecule to afford the low intensity fragment ion at *m*/*z* 277 was detected and this ion was attributed to $[M-H-H_2O]^-$ with an error of −3.97 ppm. However, the loss of H_2O was not detected for the MS^2 spectrum of $[M-H]^-$ ions of 3-AcDON and NIV. So, we assumed that the loss of H_2O for DON would occur at position C3. The MS^2 spectrum of *m*/*z* 295 (see Fig. 3(a)) contained product ion at *m*/*z* 247, which was formed by the loss of CH_4O_2 from the precursor ion. The further cleavage of epoxy at the position C-12 of the ion at *m*/*z* 247 generated the low intensity product ion at *m*/*z* 217. The product ion at *m*/*z* 205 was formed by the loss of $C_3H_6O_3$ from the precursor ion via severe cleavages. The elemental composition of the predominant product ion at *m*/*z* 138.0329 was $C_7H_6O_3$ (predicted 138.0322 Da), according to the formula predictor software, indicating that $C_7H_{11}O_2$ was lost from *m*/*z* 265 to form *m*/*z* 138. The ion at *m*/*z* 265 which was formed by the loss of CH_2O at the position C-6 from the precursor ion would form the intermediate which initially would undergo scission of the pyran rings at the bond C2–O. The structure of ion at *m*/*z* 135 might derive from the cleavage of intermediate at the bond C5–C6. The loss of C_6H_6O from *m*/*z* 217 by the cleavage of the cycle ether formed the low intensity product ion at *m*/*z* 123. The MS^3 spectrum of *m*/*z* 265 (see Fig. 3(b)) contained fragment ion at *m*/*z* 218, which was formed by the loss of CH_3O_2 from the precursor ion. The product ion at *m*/*z* 137.0585 derived an empirical formula of $C_8H_9O_2$, according to the formula predictor software, and this ion was believed to arise via the cleavage at positions C10-11 and C6-7 from *m*/*z* 218. The ion at *m*/*z* 202 was the further loss of CH_4 from the ion at *m*/*z* 218 via the intermediate of migration of the proton at C6 to the methyl. The observations described are summarized in Scheme 4 which depicts the fragmentation mechanism proposed for $[M-H]^-$ ion of DON.

As for the 3-AcDON, the product ion at *m*/*z* 247 was formed by the loss of CH_3COOH from *m*/*z* 307. The fragment pattern was confirmed by the MS^3 spectrum of precursor ion at *m*/*z* 307 (see Fig. 3(d)). The further loss of H_2O and CH_2O_2 of the ion at *m*/*z* 247

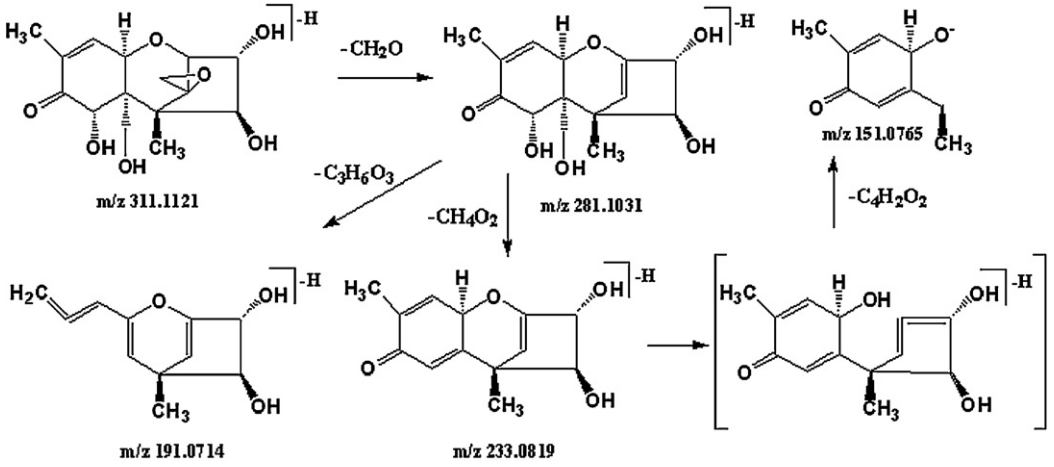

Scheme 6. The proposed fragmentation pathways for deprotonated ion $[M-H]^-$ of NIV.

Table 4
The elemental composition, accurately measured mass/charge ratio and theoretical mass/charge ratio, double bond equivalents (DBE), the mass errors expressed in milli-Daltons and parts-per-million of product ions observed in the MS^2 and MS^3 spectra for $[M-H]^-$ of DON.

Elemental composition	Measured mass/charge ratio (Th)	Theoretical mass/charge ratio (Th)	DBE	Error (mDa)	Error (ppm)
$C_{15}H_{17}O_5^-$	277.1070	277.1081	7.0	−1.1	−3.97
$C_{14}H_{17}O_5^-$	265.1073	265.1081	6.0	−0.8	−3.02
$C_{14}H_{15}O_4^-$	247.0950	247.0976	7.0	−2.6	−10.52
$C_{13}H_{14}O_3^-$	218.0911	218.0948	7.0	−3.7	−16.97
$C_{13}H_{13}O_3^-$	217.0870	217.0970	7.0	0	0
$C_{12}H_{13}O_3^-$	205.0858	205.0870	6.0	−1.2	−5.85
$C_{12}H_{10}O_3^-$	202.0684	202.0655	8.0	2.9	13.97
$C_7H_6O_3^-$	138.0329	138.0322	4.5	0.7	5.07
$C_8H_9O_2^-$	137.0585	137.0608	4.0	−2.3	−16.78
$C_7H_7O_2^-$	123.0460	123.0452	4.0	0.8	6.50

Table 5
The elemental composition, accurately measured mass/charge ratio and theoretical mass/charge ratio, double bond equivalents (DBE), the mass errors expressed in milli-Daltons and parts-per-million of product ions observed in the MS^2 and MS^3 spectra for $[M-H]^-$ of 3-AcDON.

Elemental composition	Measured mass/charge ratio (Th)	Theoretical mass/charge ratio (Th)	DBE	Error (mDa)	Error (ppm)
$C_{16}H_{19}O_6^-$	307.1187	307.1187	7.0	0	0
$C_{14}H_{15}O_4^-$	247.0978	247.0976	7.0	0.2	0.81
$C_{14}H_{13}O_3^-$	229.0905	227.0870	8.0	3.5	15.28
$C_{13}H_{13}O_2^-$	201.0931	201.0921	7.0	1.0	4.97
$C_{11}H_9O_2^-$	173.0626	173.0608	7.0	1.8	10.40
$C_9H_9O^-$	133.0688	133.0659	5.0	2.9	21.79

Table 6
The elemental composition, accurately measured mass/charge ratio and theoretical mass/charge ratio, double bond equivalents (DBE), the mass errors expressed in milli-Daltons and parts-per-million of product ions observed in the MS^2 and MS^3 spectra for $[M-H]^-$ of NIV.

Elemental composition	Measured mass/charge ratio (Th)	Theoretical mass/charge ratio (Th)	DBE	Error (mDa)	Error (ppm)
$C_{14}H_{17}O_6^-$	281.1022	281.1031	6.0	−0.9	−3.20
$C_{13}H_{13}O_4^-$	233.0826	233.0819	7.0	0.7	3.00
$C_{11}H_{11}O_3^-$	191.0756	191.0714	6.0	4.2	21.98
$C_9H_{11}O_2^-$	151.0746	151.0765	4.0	−1.9	−12.58

generated the product ions at *m*/*z* 229 and 201, respectively. In the MS^3 spectrum of precursor ion at *m*/*z* 307, the loss of $C_3H_6O_2$ and $C_5H_6O_3$ from *m*/*z* 247 formed the product ions at *m*/*z* 173 and 133, respectively. The observations described are summarized in Scheme 5 which depicts the fragmentation mechanism proposed for $[M-H]^-$ ion of 3-AcDON.

For the NIV, the low intensity product ion at *m*/*z* 233 was formed by the loss of CH_4O_2 from *m*/*z* 281. The fragment pattern was confirmed by the MS^3 spectrum of precursor ion at *m*/*z* 281 (see Fig. 3(f)). The MS^3 spectrum of *m*/*z* 281 contained product ion at *m*/*z* 191, which was formed by the loss of $C_3H_6O_3$ from the precursor ion via severe cleavages. A product ion at *m*/*z* 151.0746 derived an empirical formula of $C_9H_{11}O_2$, according to the formula predictor software, and this ion was thought to arise from the *m*/*z* 233 via the intermediate of the cleavage at positions C12-5 and C4-5. The observations described are summarized in Scheme 6 which depicts the fragmentation mechanism proposed for $[M-H]^-$ ion of NIV.

4. Conclusion

The ESI multistage tandem spectra (MS^{1-3}) with accurate masses of five trichothecenes, T-2 toxin, HT-2 toxin, DON, 3-AcDON and NIV were obtained by electrospray hybrid ion trap/time-of-flight mass spectrometry. The type-A trichothecenes were found to give strong sodium adduct ion $[M+Na]^+$. However, the type-B trichothecenes were found to give strong negative ion in the MS spectra. Based on the MS^2 and MS^3 experiments and accurate mass measurements, the fragmentation pathways for five trichothecenes were also proposed. Eliminations of isovaleryloxy group and acetic acid were the common fragmentation pathways of T-2 toxin and HT-2 toxin. However, the cleavage of epoxy was the common fragmentation pathways of DON, 3-AcDON and NIV. The substitutent group has an influence on the fragmentation of trichothecenes.

References

[1] D.W. Parry, P. Jenkinson, L. McLeod, *Fusarium* ear blight (scab) in small grain cereals––a review, Plant Pathol. 44 (2007) 207–238.
[2] Y. Ueno, in: Y. Ueno (Ed.), Trichothecenes—Chemical, Biological and Toxicological Aspects, Elsevier, Amsterdam, 1983, pp. 135–146.
[3] R. Krska, S. Baumgartner, R. Josephs, The state-of-the-art in the analysis of type-A and -B trichothecene mycotoxins in cereals, Fresenius J. Anal. Chem. 371 (2001) 285–299.
[4] V.M.T. Lattanzio, M. Pascale, A. Visconti, Current analytical methods for trichothecene mycotoxins in cereals, Trends Anal. Chem. 28 (2009) 758–768.
[5] W. Langseth, T. Rundberget, S. Uhlig, Electron ionisation mass spectrometry of the pentafluoropropionate esters of trichothecene analogues and culmorin compounds from *Fusarium* species, Rapid Commun. Mass Spectrom. 24 (2010) 2641–2649.
[6] E. Rodrigues-Fo, C.J. Mirocha, W. Xie, T.P. Krick, J.A. Martinelli, Electron ionization mass spectral fragmentation of deoxynivalenol and related tricothecenes, Rapid Commun. Mass Spectrom. 16 (2002) 1827–1835.
[7] F. Berthiller, R. Schuhmacher, G. Buttinger, R. Krska, Rapid simultaneous determination of major type A- and B-trichothecenes as well as zearalenone in maize by high performance liquid chromatography–tandem mass spectrometry, J. Chromatogr. A 1062 (2005) 209–216.
[8] M. Klotzel, B. Gutsche, U. Lauber, H.U. Humpf, Determination of 12 type A and B trichothecenes in cereals by liquid chromatography–electrospray ionization tandem mass spectrometry, J. Agric. Food Chem. 53 (2005) 8904–8910.
[9] Q. Li, G. Yan, T. Ge, A fragmentation study of podophyllotoxin and its 4′-demethyl-4β-substitute derivatives by electrospray ionization ion-trap time-of-flight tandem mass spectrometry, Rapid Commun. Mass Spectrom. 21 (2007) 2843–2852.
[10] Q. Li, G. Yan, T. Ge, A fragmentation study of two compounds related to 4′-demethylepipodophyllotoxin in negative ion electrospray ionization by MS^n ion-trap time-of-flight mass spectrometry, Rapid Commun. Mass Spectrom. 22 (2008) 373–378.